



Received on 19 August 2019; received in revised form, 23 April 2020; accepted, 26 July 2020; published 01 August 2020

FORMULATION, CHARACTERIZATION AND EVALUATION OF SOLID LIPID NANOPARTICLES OF SELECTED ANTITUBERCULAR AGENT

Mudavath Hanumanaik^{*}, K. Vinod Kumar, G. Kiran and G. Sudhakara Rao

Vishwabharti College of Pharmaceutical Sciences, Perecherla, Guntur - 522009, Andhra Pradesh, India.

Keywords:

Solid lipid nanoparticles, Rifampicin, Microemulsion Technique, ultra stirrer, Dialysis membrane's

Correspondence to Author:

Mudavath Hanumanaik

Assistant Professor,
Vishwabharti College of
Pharmaceutical Sciences, Perecherla,
Guntur - 522009, Andhra Pradesh,
India.

E-mail: m.hanumanaik7@gmail.com

ABSTRACT: The purpose of this work was to develop prolonged-release solid lipid nanoparticles (SLNs) of Rifampicin (RIF) for oral drug delivery and to improve the bioavailability of RIF. SLNs were designed by using Glycerol monostearate (GMS) and lipid core materials and polaxamer 188 as a stabilizer. SLNs were prepared by o/w microemulsion technique and characterized by particle size analysis, Fourier transforms infrared (FTIR) spectroscopy, differential scanning calorimetry (DSC), drug entrapment efficiency, scanning electron microscopy (SEM), Zeta potential, *in-vitro* evaluation studies, storage stability, membrane permeation study. At the highest speed, the resultant SLNs were smaller in size, and their size increased with an increase in lipid concentration. Nanoparticles prepared using 2.5% lipid, 1% Poloxamer 188, and 21,500 rpm show smaller particle size, better drug entrapment, excellent surface characteristic, and controlled drug release. Release from RIF-SLNs was studied using a dialysis bag method. The results of the *released in-vitro* study show that the dialysis membrane after 12 and after 24 h, the release pattern of drug slightly increases. The surface characters were found to be smooth with all the lipid carriers. Short term stability studies indicated no significant change when stored between 2-8 °C for 1 month.

INTRODUCTION: Solid lipid nanoparticles recently emerged as a novel approach to parenteral drug delivery systems. Solid lipid nanoparticles combine the advantages of lipid emulsion systems and polymeric nanoparticle systems. Utilizing biological lipids is theorized to minimize carrier cytotoxicity, and the solid-state of the lipid is theorized to permit more controlled drug release due to increased mass transfer resistance. SLNs also useful as drug carriers to treat neoplasm¹.

Mycobacterial organisms cause tuberculosis, Mycobacterium avium complex (MAC) disease, and leprosy. Tuberculosis (TB) is second only to HIV/AIDS as the greatest killer worldwide due to a single infectious agent. In 2011, 8.7 million people fell ill with TB, and 1.4 million died from TB.

Over 95% of TB deaths occur in low- and middle-income countries, and it is among the top three causes of death for women aged 15 to 44. In 2010, there were about 10 million orphan children as a result of TB deaths among parents. TB is a leading killer of people living with HIV causing one-quarter of all deaths. Multi-drug resistant TB (MDR-TB) is present in virtually all countries surveyed². The rifamycins (rifampin, rifabutin, rifapentine) are a group of structurally similar, complex macrocyclic antibiotics produced by

<p>QUICK RESPONSE CODE</p> 	<p>DOI: 10.13040/IJPSR.0975-8232.11(8).3734-44</p> <hr/> <p>The article can be accessed online on www.ijpsr.com</p> <hr/> <p>DOI link: http://dx.doi.org/10.13040/IJPSR.0975-8232.11(8).3734-44</p>
---	--

Amycolatopsis mediterranei rifampin (RIFADIN; RIMACTANE) is a semi-synthetic derivative of one of these rifamycin B. Rifampin inhibits DNA-dependent RNA polymerase of mycobacteria and other microorganisms by forming a stable drug-enzyme complex, leading to suppression of initiation of chain formation (but not chain elongation) in RNA synthesis Rifampicin posses protein binding of 89% and shorter half-life 1-5 h which gets well absorbed from the gastrointestinal tract with bioavailability varied from 90-953,⁴.

The present study is aimed at the development and characterizations of SLNs of RIF. SLNs prepared by the Microemulsion technique yield SLNs with good drug loading capacity and are possible to alter the therapeutic index and the duration of activity of drugs. The process of formation of these SLNs is simple with high reproducibility and safe as biodegradable lipid carriers Glyceryl monostearate (GMS); the surfactants are used like poloxamer 188, which produced chemically stabled system.

MATERIALS AND METHODS: Rifampicin was obtained as a gift sample from Novartis-Sandoz, Pvt. Ltd, Maharashtra. Glycerol Monostearate were procured from Loba Chemicals, Pvt. Ltd, Mumbai. Polaxamer-188 was obtained from S.D. Fine Chem Ltd., Mumbai. The dialysis membrane was purchased from Himedia Laboratories Pvt. Ltd., Mumbai. All the chemicals which were used of either pharma or analytical grade.

Formulation Design:

Procedure for Preparation of SLN'S by Microemulsion Technique: SLNs were prepared from o/w microemulsion technique containing lipid (GMS) carrier, polaxamer 188 as a surfactant. GMS was added dropwise maintained at 70 °C into ice-cold water (2-3 °C) with continuous stirring (IKA-Ultra Turrax T25 USA) to form SLNs. The samples were sonicated and analyzed for particle size^{5, 6}. The details of Formulation Designs are tabulated in **Table 1**.

TABLE 1: FORMULATION DESIGN OF RIF LOADED GMS SLNS

Formulation Codes	Lipid %W/V	Drug (mg)	Conc. Of Surfactant W/V	Speed (rpm)
Lipid concentration (%)				
FGL-01	2.5%	10 mg	1%	9,500
FGL-02	5.0%	10 mg	1%	9,500
FGL-03	7.5%	10 mg	1%	9,500
FGL-04	10.0%	10 mg	1%	9,500
Surfactant concentration (%)				
FGP-05	2.5%	10 mg	1%	9,500
FGP-06	2.5%	10 mg	1.5%	9,500
FGP-07	2.5%	10 mg	2%	9,500
FGP-08	2.5%	10 mg	2.5%	9,500
Speed of ultra stirrer (rpm)				
FGS-09	2.5%	10 mg	1%	9,500
FGS-10	2.5%	10 mg	1%	13,500
FGS-11	2.5%	10 mg	1%	17,500
FGS-12	2.5%	10 mg	1%	21,500

FGL- Formulation of GMS with changing lipid conc., FGP- Formulation of GMS with changing Poloxamer conc., FGS- Formulation of GMS with changing speed

Evaluation of SLNs:

Compatibility Studies of Drug and Polymers:

Compatibility studies of drugs and polymers were done by FTIR spectrophotometer (Thermo Nicolet, Japan).

The infrared spectra of the drug and polymers were run individually. Then it was investigated for any possible interaction between polymer and drug. IR spectral data are shown in Spectra and tabulated in **Table 2**.

Differential Scanning Calorimetry (DSC):

studies are also a qualitative identification of the substance in the pure form and in combination. DSC was carried by the action of Argon purging with 80 ml/min, where it is hermetically sealed with Aluminium Pans, from this sample of 40 µl is used. The program is run at 25-250 °C. The onset, end set, and the peaks are recorded for individual pure drug, lecithin, and formulations. The spectra are shown in spectra⁹⁻¹². The peaks values are tabulated in **Table 3**.

TABLE 2: DATA OBTAINED FROM COMPATIBILITY STUDY OF DRUG POLYMER AND FORMULATIONS BY FTIR SPECTROSCOPY

S. no.	Polymer/Drug	Important IR Spectral peaks of different groups, wavelength in cm ⁻¹			
		OH Stretch	CH Stretch(Aliphatic)	C=O Stretch	C--O—C Stretch
1	Rifampin	3438.32	2925.78	1724.47	1151.85
2	Glycerylmonosterate(GMS)	3625.37	2850.02	1735.29	1185.24
3	Rifampin : GMS	3625.37	2850.02	1739.06	1049.63

TABLE 3: DATA OBTAINED FROM COMPATIBILITY STUDY OF DRUG AND POLYMER BY DIFFERENTIAL SCANNING CALORIMETRY

S. no.	Drug/Polymer/ Formulation	Peaks
1	Pure Rifampin	183 °C (Rifampin)
2	Rifampin : Glyceryl Monosterate	58.4 ^o C (Glyceryl Monosterate) 182.1 °C (Rifampin)

Particle Size Analysis: The nanotracer measurement technique is that of dynamic light scattering. The velocity distribution of a sample particle suspended in a dispersing medium is a known function of particle size. Light from a laser diode is coupled to the sample through an optical power splitter/probe assembly. Light scattered from each particle is Doppler-shifted by the particle motion (Brownian motion). The Doppler-shifted scattered light is mixed with coherent un-shifted light in a silicon photo-detector and down-converted to the audio range. The detector output signal is then amplified, filtered, digitized, and mathematically analyzed by the Microtrac windows software. Clean the cell with Mineral Water.

Check the background (BVG should not cross than 0.1) then Add Mineral Water and Set Zero. 5 ml Sample was inserted into sample cell with a pipette. And Allow 10 cycles RUN to measure size⁷.

Scanning Electron Microscopy:

Procedure: The surface morphology of the specimens will be determined by using a scanning electron microscope (SEM), Model JSM 840A, JEOL, Japan. The samples are dried thoroughly in vacuum desiccator before mounting on brass specimen studies, using double-sided adhesive tape. Gold-palladium alloy of 1200A was coated on the sample using a sputter coating unit (Model E5 100 Polaron U.K.) in Argon at an ambient of 8-10 Pascal with plasma voltage about 20 MA. The sputtering was done for nearly 5 min to obtain uniform coating on the sample to enable good

quality SEM images. The SEM was operated at a low accelerating voltage of about 15 KV with a load current of about 80MA. The condenser lens position was maintained between 4.4-5.1. The objective lens aperture has a diameter of 240 microns and the working distance WD = 39 mm⁸.

Entrapment Efficiency: Entrapment efficiency of RIF-SLNs was determined by centrifugation of samples at 10,000 rpm for 10 min. The amount of free drug was determined in the clear supernatant by UV spectrophotometer (Thermospectronic Genesys-6. USA) at 479.5 nm using the supernatant of non loaded nanoparticles on the basic correction. The entrapment efficiency (EE %) could be achieved by the following equation⁹.

$$EE (\%) = \frac{W_{\text{initial drug}} - W_{\text{free drug}}}{W_{\text{initial drug}}} \times 100$$

Short Term Stability Study: The short term stability of the SLNs was studied below 2-8 °C. The SLNs were evaluated at 2-8 °C for a period of 1 month. The samples were observed for particle size analysis, To, Entrapment efficiency, and *in-vitro* release studies¹⁰.

Zeta Potential: The particle charge is one of the factors that determine the physical stability of emulsions and suspensions. The higher is the electrostatic repulsion between the particles, the higher is the physical stability.

Typically the particle charge is quantified as the so-called zeta potential, which is measured by using Zeta meter (Malvern Instruments Ltd., UK); about 1 ml of SLN was dispersed in 1 ml of distilled water by sonication, and it was subjected to Zeta potential analyzer¹¹.

In-vitro Release Study: *In-vitro* release studies were performed using the dialysis bag diffusion technique. Dialysis membrane (molecular weight - 12,000 Da) was soaked in double-distilled water for 12 h before use for the experiment. RIF nano-suspension equivalent to 1 mg of RIF was placed in

the dialysis bag containing 50 mL of dissolution medium at 37 ± 0.5 °C with continuous magnetic stirring at 200 rpm. At fixed time intervals, the samples were withdrawn; the same dissolution medium was replaced by a fresh medium to

maintain a constant volume. Sink conditions were maintained for release studies. Samples were analyzed by UV visible spectroscopy at 479.5 nm. The results are shown in **Graph 16-18**, and their values are tabulated in **Table 17-19**¹².

TABLE 4: MEAN PARTICLE SIZE RANGE OF SLNS OF RIF BY USING GMS AS A LIPID CARRIER AND POLOXAMER 188 AS SURFACTANTS

Formulation code	FGL-01	FGL-02	FGL-03	FGL-04	FGP-05	FGP-06	FGP-07	FGP-08	FGS-09	FGS-10	FGS-11	FGS-12
Avg. Particle size (nm)	366	451	397	342	366	342	316	431	320	234	226	112

TABLE 5: DRUG ENTRAPMENT EFFICIENCY WITH GMS AS A LIPID CARRIER:

Formulation code	FGL-01	FGL-02	FGL-03	FGL-04	FGP-06	FGP-07	FGP-08	FGS-10	FGS-11	FGS-12
Drug entrapment efficiency	61.20%	72.00%	78.25%	82.20%	56.21%	52.16%	47.60%	59.75%	57.00%	54.86%

FGL- Formulation of GMS with changing lipid conc., FGP- Formulation of GMS with changing Poloxamer conc., FGS- Formulation of GMS with changing speed

TABLE 6: COMPARATIVE IN-VITRO DRUG RELEASE STUDY OF GMS NANOPARTICLES OF RIF

Time/formulation code	% Cumulative drug release (CDR)					
	2h	4h	6h	8h	10h	12h
FGL-01	17.3256	26.6647	36.2485	45.5896	61.2569	71.2639
FGL-02	14.5641	21.5142	29.3368	40.2269	53.5683	63.7569
FGL-03	11.7859	18.2078	28.3501	38.0369	50.4469	60.0863
FGL-04	08.6982	15.9936	23.7386	35.0364	46.5695	55.5574
FGP-06	19.2135	29.8803	40.2589	55.2156	63.2456	76.4871
FGP-07	21.2898	32.6787	46.3367	61.2034	72.0314	83.1587
FGP-08	24.4431	34.5896	48.9248	63.01875	76.5479	88.4103
FGS-10	18.1942	29.0456	39.3201	47.5367	64.7378	76.5741
FGS-11	21.1304	30.5763	42.3894	52.9739	66.7466	78.5896
FGS-12	24.6201	33.2668	45.8063	56.9014	72.6947	85.8933

FGL- Formulation of GMS with changing lipid conc., FGP- Formulation of GMS with changing Poloxamer, FGS- Formulation of GMS with changing speed

TABLE 7: DATA ANALYSIS KINETIC DATA OF VARIOUS MODELS FOR RELEASE STUDY (GMS)

Formulation Code	Zero order		First order		Higuchi		Peppas			Best fitting Model
	R	K	R	k	R	K	R	k	N	
FGL-01	0.9821	5.724	0.9619	-0.043	0.930	20.14	0.9941	0.7920	0.2436	Peppas
FGL-02	0.9600	5.5444	0.9059	-0.041	0.870	19.00	0.9801	0.8702	0.2386	Peppas
FGL-03	0.9702	5.5551	0.8826	-0.040	0.843	18.78	0.9752	0.9887	0.2339	Peppas
FGL-04	0.9923	4.6690	0.9679	-0.029	0.873	15.93	0.9955	1.0524	0.2391	Peppas
FGP-06	0.9913	6.1225	0.9685	-0.049	0.944	21.76	0.9916	0.7747	0.2374	Peppas
FGP-07	0.9910	6.7764	0.9673	-0.062	0.951	23.89	0.9939	0.776	0.2697	Matrix
FGP-08	0.9856	7.1047	0.9387	-0.073	0.995	25.36	0.9854	0.7356	0.2348	Peppas
FGS-10	0.9807	6.0946	0.9455	-0.049	0.922	21.45	0.9923	0.7931	0.2349	Peppas
FGS-11	0.9812	6.2392	0.9588	-0.052	0.945	22.19	0.9906	0.7387	0.2745	Peppas
FGS-12	0.9438	6.7403	0.9259	-0.065	0.946	23.99	0.9867	0.7045	0.2878	Peppas

TABLE 8: DATA FOR OPTIMIZE FORMULATION TABLE

Formulation Codes	Lipid %W/V	Conc. Of Surfactant W/V	Speed (rpm)
FRG-4	10%	1%	9,500

TABLE 9: EVOLUTION DATA FOR OPTIMIZED FORMULATION

Batch	FRG-4
Parameters	
Particle size	271
% E.E	68

FRG- Optimize formulation of RIFSLNs with GMS lipid

Data Analysis: The Colloidal systems were reported to follow the zero-order release rate by the

diffusion mechanism for the release of the drug. To analyze the mechanism for the release and release rate kinetics of the dosage form, the data obtained was fitted into Zero order, First order, Higuchi matrix, and Korsmeyer and Peppas model.

Using PSP-DISSO-v2 software. Comparing the r-values obtained, the best-fit model was selected.

TABLE 10: IN-VITRO DRUG RELEASE STUDY FOR OPTIMIZED FORMULATION (FG-4)

Time	Abs	Conc.	DR	CLA	CDR	% CDR	CDR % retained
1	0.022	0.77	0.0385	0	0.03927	3.927	96.073
2	0.032	1.33	0.0665	0.00133	0.06783	6.783	93.217
3	0.049	2.27	0.1135	0.00227	0.11577	11.577	88.423
4	0.060	2.88	0.144	0.00288	0.13688	13.688	86.312
5	0.066	3.22	0.161	0.00322	0.15422	15.422	83.578
6	0.069	3.38	0.169	0.00338	0.17238	17.238	82.762
7	0.074	3.66	0.183	0.00366	0.1866	18.66	81.34
8	0.080	4.00	0.2	0.004	0.214	21.4	78.6
9	0.084	4.22	0.211	0.00422	0.23522	23.522	76.478
10	0.099	5.05	0.2525	0.00505	0.2575	25.75	74.25
11	0.124	6.444	0.3222	0.00644	0.28866	28.866	71.134
12	0.149	7.833	0.3916	0.00783	0.3292	32.92	67.08
24	0.221	11.83	0.5915	0.01183	0.3933	39.33	60.07

Equivalent Amount of Drug in SLNs = 1 mg, Volume of dissolution medium = 50 ml pH 1.2+ 6.8 phosphate buffer, FG-4 Formulation with GMS

TABLE 11: MEAN PARTICLE SIZE RANGE OF SLNS AFTER 1 MONTH OF STORAGE AT 2-8 °C

S. no.	Formulation Code	Mean Particle Size (Nm) (Before Storage)	Mean Particle Size (Nm) (After Storage)
1	FG-4	342	347

TABLE 12: DRUG ENTRAPMENT EFFICIENCY OF SLNS AFTER 1 MONTH OF STORAGE AT 2-8 °C

S. no.	Formulation Code	Drug Entrapment Efficiency (before storage)	Drug Entrapment Efficiency (after storage)
1	FG-4	82 %	86 %

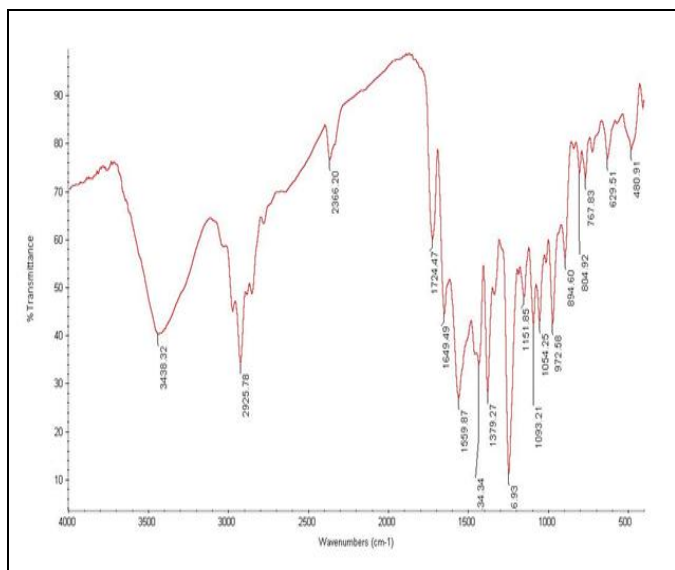
TABLE 13: IN-VITRO DRUG RELEASE PROFILE AFTER 1 MONTH OF STORAGE OF SELECTED FORMULATION (FG-4) AT 2-8 °C

Time (hrs)	Absorbance	Conc. (mcg/ml)	Drug Release	CLA	Cum Drug Release	% Cum Drug Release	CDR % retained
1	0.025	0.944444	0.047222	0	0.047222	4.722222	95.2778
2	0.036	1.555556	0.077778	0.001556	0.079333	7.933333	92.0667
3	0.051	2.388889	0.119444	0.002389	0.121833	12.18333	87.8167
4	0.063	3.055556	0.152778	0.003056	0.155833	15.58333	84.417
5	0.067	3.277778	0.163889	0.003278	0.167167	16.71667	83.2834
6	0.072	3.555556	0.177778	0.003556	0.181333	18.13333	81.8667
7	0.075	3.722222	0.186111	0.003722	0.209833	20.98333	81.017
8	0.082	4.111111	0.205556	0.004111	0.239667	23.96667	79.0167
9	0.085	4.277778	0.213889	0.004278	0.248167	24.81667	75.1834
10	0.102	5.222222	0.261111	0.005222	0.276333	27.63333	72.3667
11	0.126	6.555556	0.327778	0.006556	0.319	31.9	68.1
12	0.15	7.888889	0.394444	0.007889	0.33255	33.255	66.745

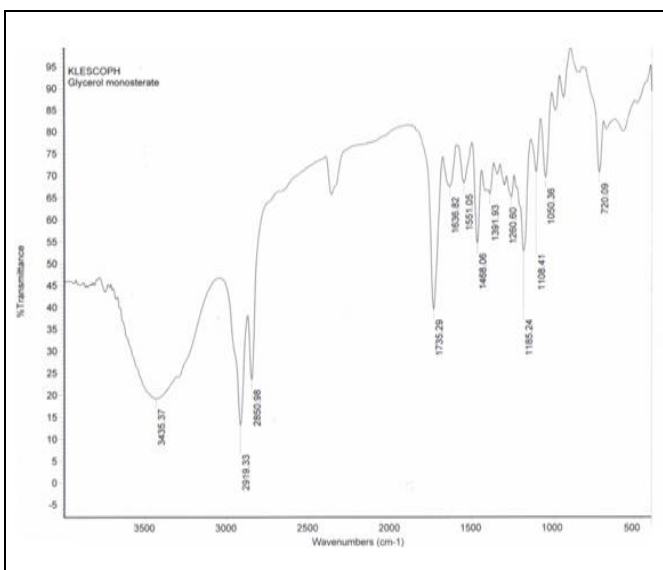
Equivalent Amount of Drug in SLNs = 1 mg, Volume of dissolution medium = 50 ml pH 1.2+6.8 phosphate buffer, FG-4 storage of formulation with GMS

TABLE 14: % CDR FROM SLNs AFTER 1 MONTH OF STORAGE AT 2-8 °C

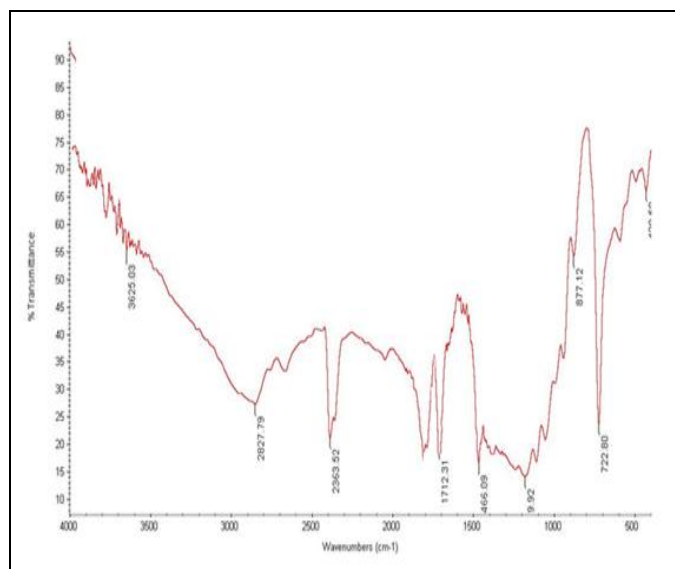
S. no.	Formulation Code	% CDR (before storage)	% CDR (after storage)
1	FG-4	32.92	33.255



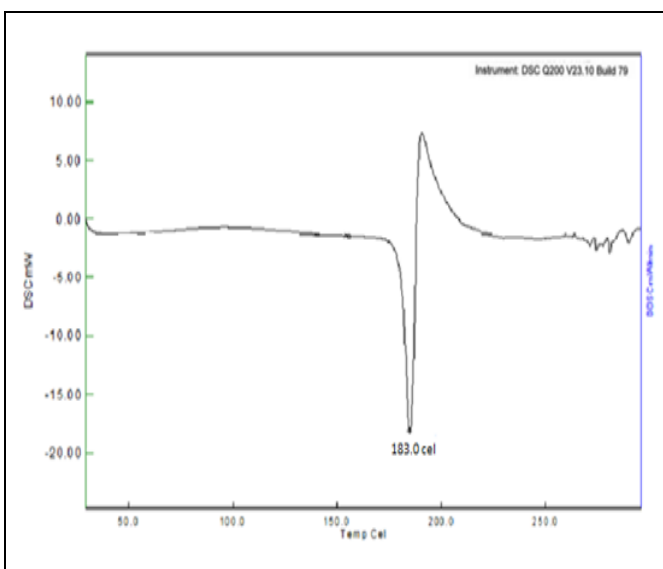
SPECTRA 1: FTIR SPECTRA OF RIFAMPICIN



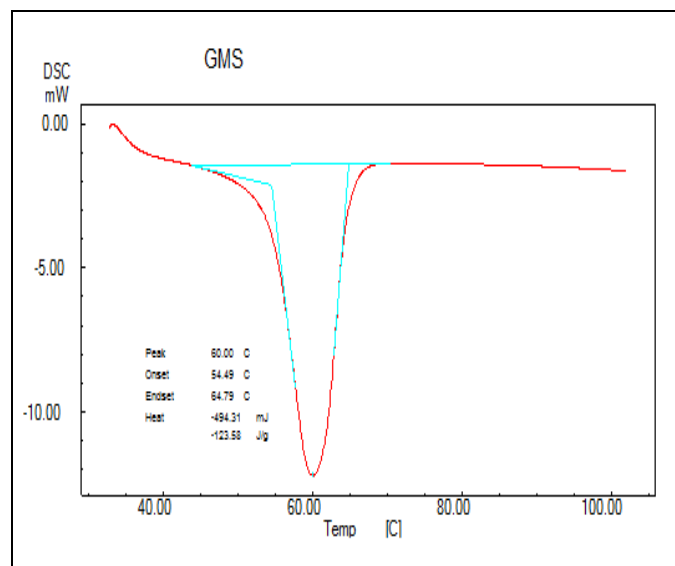
SPECTRA 2: FTIR SPECTRA OF GMS



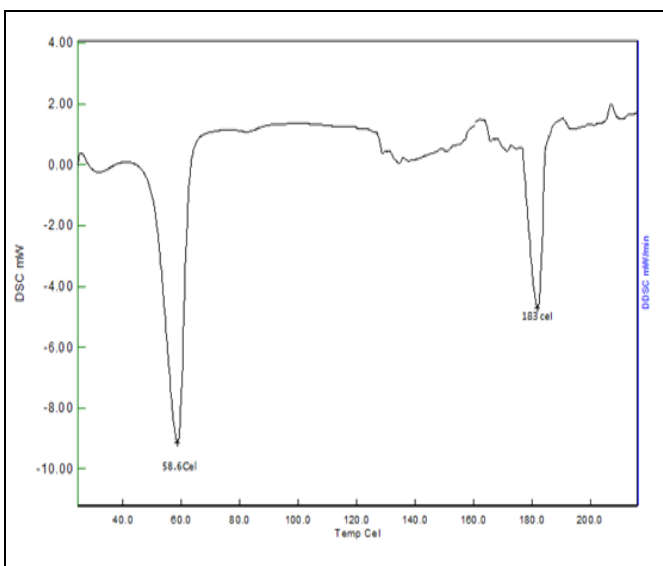
SPECTRA 3: FTIR SPECTRA OF RIFAMPICIN: GMS



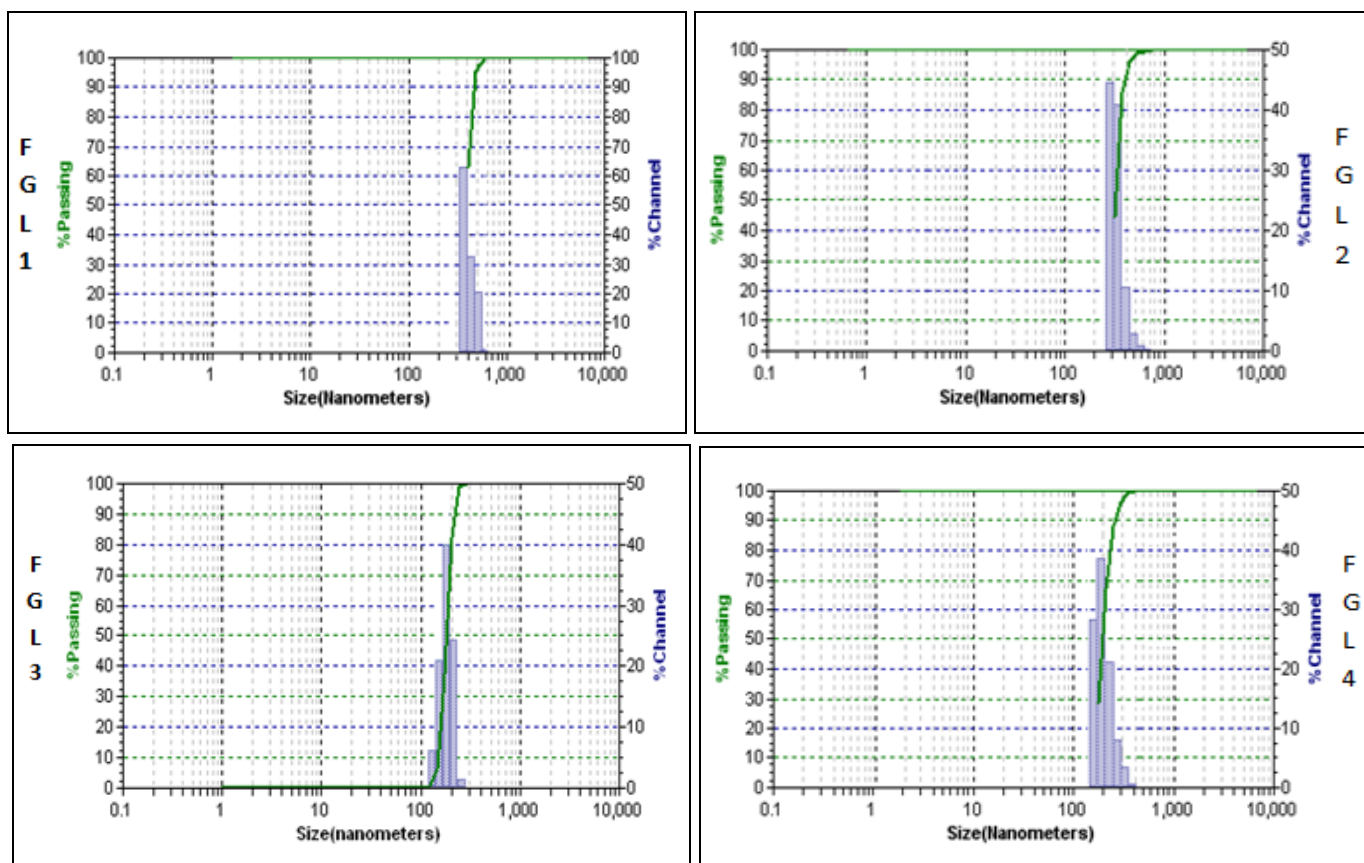
SPECTRA 4: DSC SPECTRA OF RIFAMPICIN



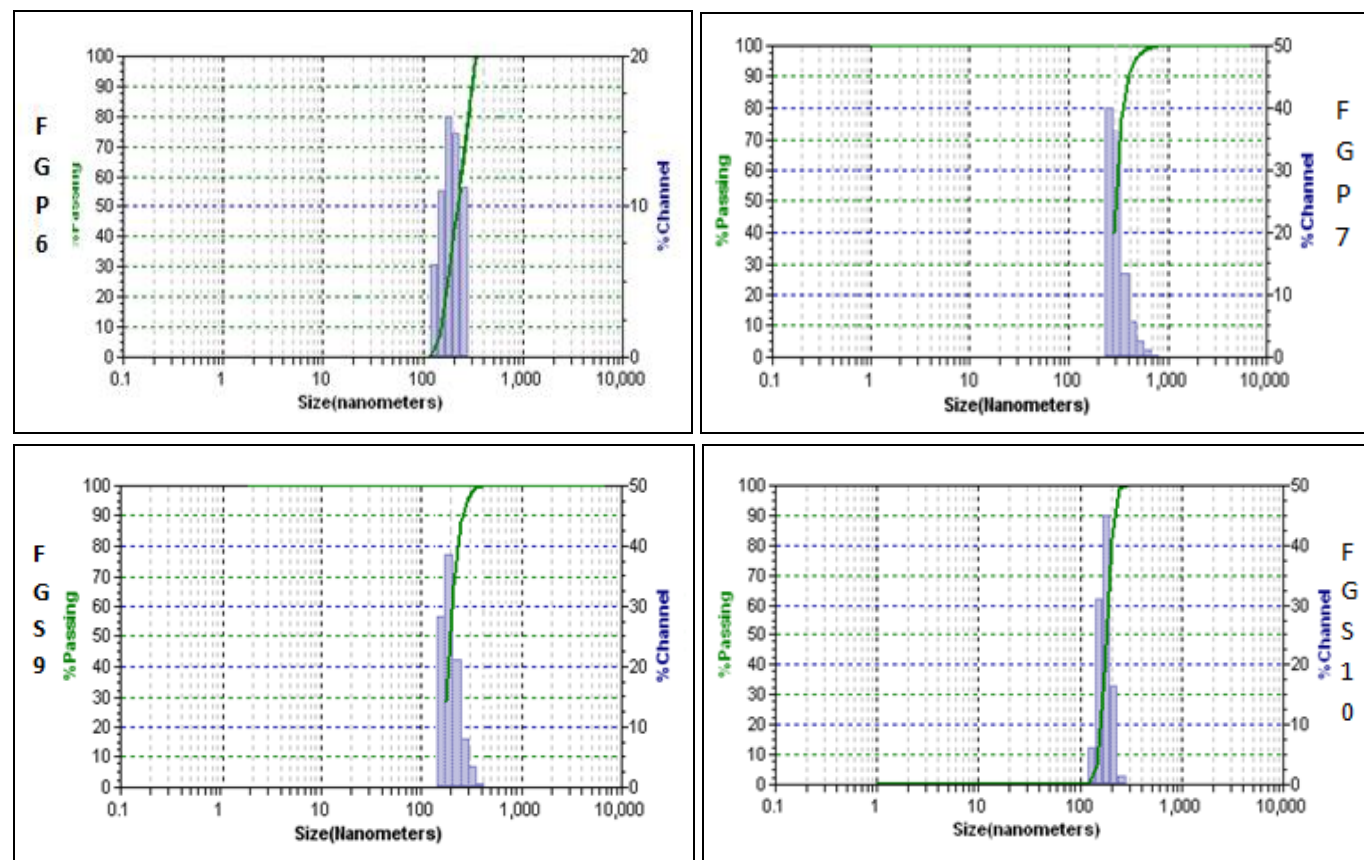
SPECTRA 5: DSC SPECTRA OF GLYCERYL MONOSTERATE



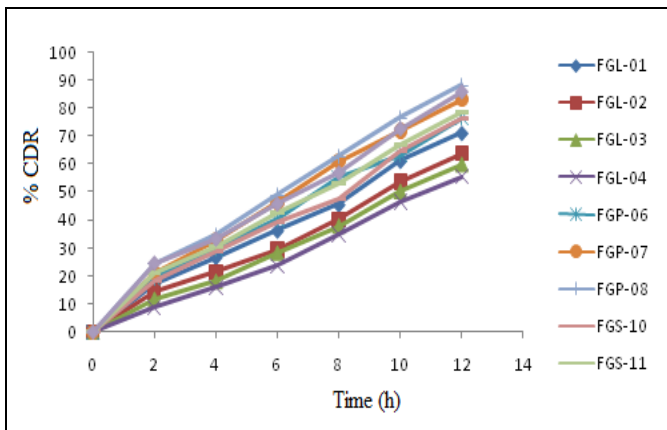
SPECTRA 6: DSC SPECTRA OF RIFAMPICIN: GLYCERYL MONOSTERATE



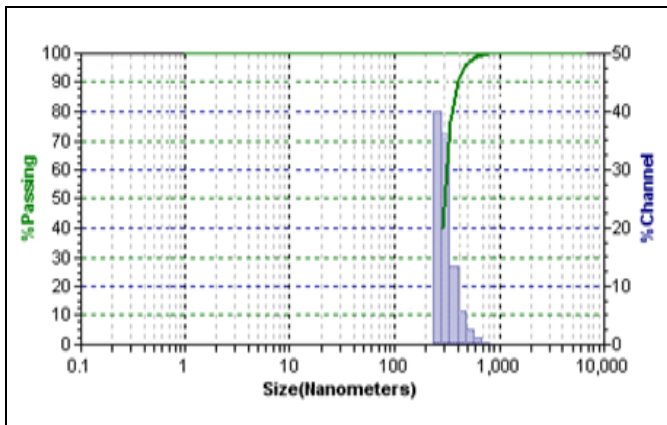
GRAPH 1: PARTICLE SIZE RANGE OF SLNS WITH RIF BY USING GMS [VARIABLES: LIPID AND POLOXAMER CONCENTRATION (%)]



GRAPH 2: PARTICLE SIZE RANGE OF SLNS WITH RIF BY USING GMS [VARIABLES: POLOXAMER CONCENTRATION (%) AND SPEED OF ULTRA STIRRER]



GRAPH 3: IN-VITRO DRUG RELEASE PROFILE OF FG-1 TO FG-12 FGL- Formulation of GMS with changing lipid conc., FGP- Formulation of GMS with changing Poloxamer conc., FGS- Formulation of GMS with changing speed



GRAPH 4: FRG4- OPTIMIZE FORMULATION OF RIFSLNS WITH GMS LIPID

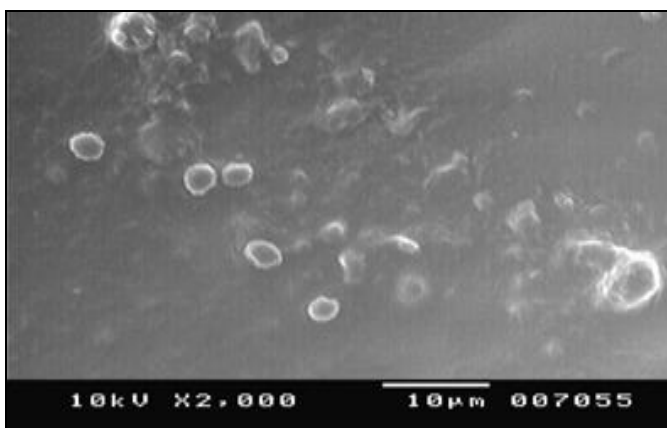


FIG. 1: SEM REPORT OF OPTIMIZED BATCHES OF RIFAMPICIN LOADED S FG-4 Formulation with Glyceryl mono stearate

Zero Order Kinetics: Drug dissolution from pharmaceutical dosage forms that do not disaggregate and release the drug slowly, assuming that the area does not change and no equilibrium conditions are obtained can be represented by the following equation –

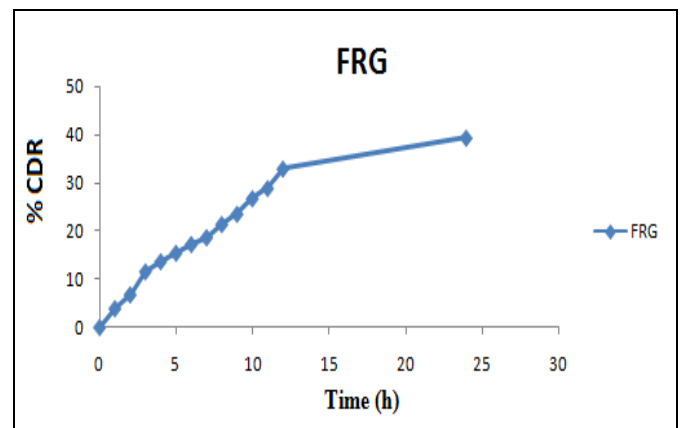
$$Q_t = Q_0 + K_0 t$$

Where Q_t = amount of drug dissolved in time t , Q_0 = initial amount of drug in the solution and K_0 = zero-order release constant.

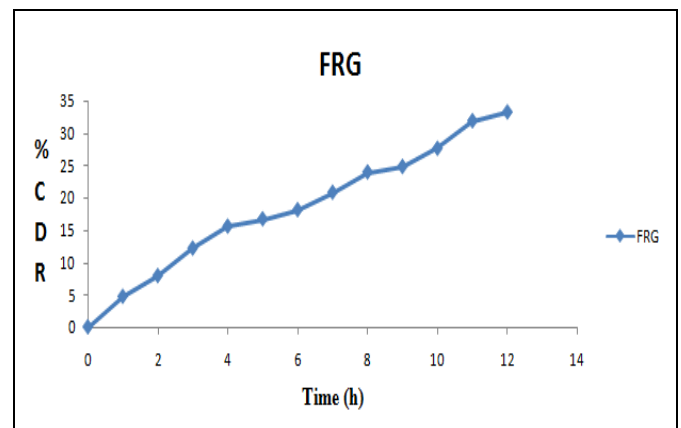
First Order Kinetics: To study the first-order release rate kinetics, the release rate data were fitted to the following equation.

$$\text{Log } Q_t = \text{log } Q_0 + K_1 t / 2.303$$

Where Q_t is the amount of drug released in time t , Q_0 is the initial amount of drug in the solution, and K_1 is the first-order release constant.



GRAPH 5: COMPARATIVE IN-VITRO DISSOLUTION STUDY OF OPTIMIZE FORMULATIONS FG- 4storage of formulation with gms



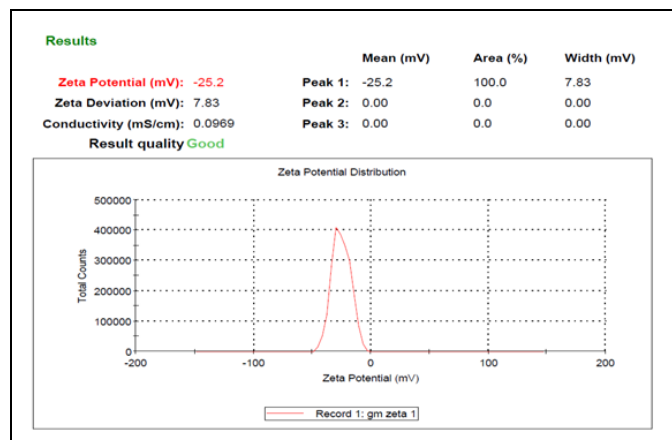
GRAPH 6: DRUG RELEASE PROFILE AFTER 1 MONTH OF STORAGE OF SELECTED FORMULATION OPTIMIZED FORMULATIONS (FG-4) FG- 4 storage of formulation with GMS

Higuchi Model: Higuchi developed several theoretical models to study the release of water-soluble and low soluble drugs incorporated in semisolids and or solid matrices. Mathematical expressions were obtained for drug particles

dispersed in a uniform matrix behaving as the diffusion media, the equation is

$$Q_t = K_H \cdot t^{1/2}$$

Where Q_t = Amount of drug released in time t , K_H = Higuchi dissolution constant.



GRAPH 7: ZETA POTENTIAL OF GMS (FG-4)

Korsmeyer and Peppas Release Model: To study this model the release rate data are fitted to the following equation

$$M_t / M_\infty = K \cdot t^n$$

Where M_t / M_∞ is the fraction of drug release, K is the release constant, t is the release time, and n is the Diffusion exponent for the drug release that is dependent on the shape of the matrix dosage form.

Hixson- Crowell Model: To study the Hixson – Crowell model the release rate data are fitted to the following equation

$$W_0^{1/3} - W_t^{1/3} = Kst$$

Where, W_0 is the amount of drug in the dosage form, W_t is the remaining amount of drug in the pharmaceutical dosage form, Ks is a constant incorporating the surface-volume relationship¹³.

RESULTS AND DISCUSSION:

Compatibility: From the I.R. spectral analysis it was found that I.R. spectrum Rifampicin with lipids (GMS) showed all characteristic peaks in combination with no significant changes as shown in **Table 2**.

DSC studies indicate that, thermal peak of Rifampicin in the pure form was identical with physical mixtures; this indicates that there is no

interaction in the formulation. (Spectra 4, 5, 6 and **Table 3**)

Formulation of RIF loaded SLNs: RIF loaded SLNs were successfully prepared by using o/w micro-emulsion technique. The SLNs were obtained immediately when dispersing the warm micro-emulsion into cold water with the aid of a homogenizer. The cold water facilitated rapid lipid crystallization and prevented lipid aggregation. Different lipid carriers were used like GMS and cetyl palmitate along with mixtures of surfactants.

Evaluation of SLNs:

Particle Size: The particle sizes of all formulations were listed in **Table 16 to 19**, and the size distribution graphs were showed in 4 Particle size of nanoparticles of Rifampicin was found to be GMS such as FGL-1 to FGS-8 showed wide distribution in particle size ranging from 112 nm to 306 nm. The particle size analysis reveals that the size reduction was with varying speeds and size increment with varying lipid carrier concentrations.

Influence of Speed (rpm) on SLN: Decreasing the particle size with the increasing of stirring rate can be explained by the intensification of the micro mixing (*i.e.*, mixing on the molecular level) between the multi-phases. High micromixing efficiency enhanced the mass transfer and the rate of diffusion between the multiphase, which induced high homogenous supersaturation in a short time and thus rapid nucleation to produce smaller drug particles. Hence, a higher stirring rate favored the formation of the smaller and more uniform drug particles.

Influence of Lipid Concentration on SLN: As the lipid concentration was increased, more particles were aggregated, resulting in a decreased yield. The yield was <50% at lipid concentration of 2.5% and dropped to the 5% range when the lipid concentration exceeded 10%.

When the concentration of the lipid exceeded 1.0% with a fixed concentration of Surfactants, there were insufficient surfactants available to coat the surface of all the lipid droplets, resulting in particle aggregation and an increase in particle size.

Entrapment Efficiency: The formulations prepared with GMS (47% to 82%), respectively.

The entrapment efficiencies of the RIF loaded SLNs were in the order of FG. The higher entrapment efficiency with Rifampicin is attributed to the high hydrophobicity due to the long-chain fatty acids attached to the triglyceride resulting in increased accommodation of lipophilic drugs.

In-vitro Dissolution Studies: *In-vitro* drug release data from the SLNs were carried out for 12 h and graphically represented as % CDR v/s time profile. The Cumulative Percent drug released after 12 h FG-1 to FG-8 was 38.32 to 75.26% for respectively.

Interestingly, the particle size had no influence on the *in-vitro* release of RIF. The release of a drug from the SLN can be influenced by the nature of the lipid matrix and its concentration. Since the surfactant concentration was optimized at 1% in the present investigation, the drug release profile was affected by other parameters such as lipid nature, the solubility of the drug in lipid, and partition coefficient. In such a model, the drug enriched core is surrounded by a practically drug-free lipid shell.

Due to the increased diffusion distance and hindering effects by the surrounding solid lipid shell, the drug has a controlled release profile. The GMS had shown slow release, which can be attributed to the hydrophobic long-chain fatty acids of the triglyceride that retain lipophilic drugs.

Kinetic Study: The release study was further investigated for the kinetic studies. Various kinetic models were applied, and their values were noted. Almost all formulations (with different lipid carriers) were found to follow the Peppas model. From the n values obtained it can be said that the diffusion followed non-Fickian mechanism.

Optimization Results: On the basis of low particle size, high entrapment efficiency and control of release profile, We selected each best formulation as optimized from a different type of lipids formulation (FG-12) the selected optimized formulation was subjected for further evaluation.

SEM: The smooth surface of SLNs is because of the presence of polaxamer 188. The surface morphology of the SLNs had not been altered by the type of lipid carrier, the concentration of lipid carrier, and speed.

Short Term Stability Studies: The selected formulations (one from each set) was stored at 2-8 °C for a month. There was no significant change of particle size, entrapment efficiency, and *in-vitro* drug release. The reason for good stability was the use of emulsifying agents appears to produce mixed surfactant films at the interface having high surfactant coverage as well as sufficient viscosity to promote stability.

Zeta Potential: In general, particle aggregation is less likely to occur for charged particles (high Zeta potential) due to electric repulsion. Lower zeta potential facilitates aggregation. The Zeta potential of both lipid-based nanoformulations was found to be -25.2, which will not allow aggregation

CONCLUSION: RIF loaded SLNs can be successfully formulated from Microemulsion Technique to enhance the efficacy of the drug by reducing the side effects from the dose. The optimized SLNs formulations of RIF showed particle sizes in the range of 271 nm-440 nm; with good surface characters.

Increment in particle size was observed with increased concentrations of lipid carriers. The smaller size was obtained with increasing stirring speed. Interestingly, the particle size had no influence on the *in-vitro* drug release was observed. Glyceryl monostearate had shown controlled release and maximum entrapment efficiency, which can be attributed to the hydrophobic long-chain fatty acids of the triglyceride that retain lipophilic drugs and also increased accommodation of lipophilic drugs.

The study reveals the influence of formulation parameters (concentration of surfactant, concentration of lipid carrier) and process parameters (stirring speed) on the entrapment efficiency and *in-vitro* release of a lipophilic drug.

ACKNOWLEDGEMENT: Authors are thankful to secretary correspondent, Principal of Vishwabharti College of Pharmaceutical Sciences Perecherla, Guntur, Andhra Pradesh, for providing necessary facilities to carry out this work. I am thankful to Novartis-Sandoz, Pvt. Ltd, Maharashtra, for providing gift samples of Rifampicin, respectively.

CONFLICTS OF INTEREST: Nil

REFERENCES:

1. Wong HL, Bendayan R, Rauth AM, Yongqiang L and Xiao YW: Chemotherapy with anticancer drugs encapsulated in solid lipid nanoparticles. *Advanced Drug Delivery* 2007; 59: 491-04. Richard DH and Mary JM. *Pharmacology* ed. 3rd Indian ed: Lippincot Williams & Wilkins Publishers; 2006.
2. WWW.WHO.COM
3. Farr BF: Rifamycins. In, Mandell, Douglas and Bennett's Principles and Practice of Infectious Diseases, ed. 5th (Mandell, GL, Bennett, JE, and Dolin, R., eds.) Churchill Livingstone, Philadelphia 2000; 348-61.
4. Vernon AA: Rifamycin antibiotics, with a focus on newer agents. In, Tuberculosis, 2nd ed. (Rom, W.N and Gray, S.M., eds.) Lippincott, Williams and Wilkins, Philadelphia, 2004; 759-71.
5. Tiyafoonchai W, Tungpradit W and Plianbangchang P: Formulation and characterization of curcuminoids loaded solid lipid nanoparticles. *International Journal of Pharmaceutics* 2007; 337: 299-06.
6. Rainer HM, Karsten M and Sven G: Solid lipid nanoparticles (SLN) for controlled drug delivery-a review of the state of the art. *European Journal of Pharmaceutics and Biopharmaceutics* 2000; 50: 161-77.
7. Morel S, Ugazio E, Cavalli R and Gasco MR: Thymopentin in solid lipid nanoparticles. *Int J Pharm* 1996; 132: 259-61.
8. Venkateswarlu V and Manjunath K: Preparation, characterization and *in-vitro* release kinetics of clozapine solid lipid nanoparticles. *J Control Release* 2004; 95(3): 627-38.
9. Dubes A, Lopez HP, Abdelwahed W, Degobert G, Fessi H, Shahgaldian P and Coleman AW: Scanning electron microscopy and atomic force microscopy imaging of solid lipid nanoparticles derived from amphiphilic cyclodextrins. *European Journal of Pharmaceutics and Biopharmaceutics* 2003; 55(3): 279-82.
10. Nguyen A, Marsaud V, Bouclier C, Top S, Vessieres A, Pigeon P, Gref R, Legrand P, Jaouen G and Jack-Michel R: Nanoparticles loaded with ferrocenyl tamoxifen derivatives for breast cancer treatment. *Int J Pharm* 2007; 06(033): 1-27.
11. Khalil Mitri: Lipid nanocarriers for dermal delivery of lutein: Preparation, characterization, stability and performance. *Int Journal of Pharma* 2011; 414: 267-75.
12. Paulo C and Jose MSL: Modelling and comparison of dissolution profiles. *Eur J Pharm Sci* 2001; 13: 123-31.
13. J Liu, Hu W, Chen H, Ni Q, Xu H and Yang X: Isotretinoin-loaded solid lipid nanoparticles with skin targeting for topical delivery. *Int J Phar* 2007; 328: 191-5.

How to cite this article:

Hanumanaik M, Kumar KV, Kiran G and Rao GS: Formulation, characterization and evaluation of solid lipid nanoparticles of selected anti-tubercular agent. *Int J Pharm Sci & Res* 2020; 11(8): 3734-44. doi: 10.13040/IJPSR.0975-8232.11(8).3734-44.

All © 2013 are reserved by the International Journal of Pharmaceutical Sciences and Research. This Journal licensed under a Creative Commons Attribution-NonCommercial-ShareAlike 3.0 Unported License.

This article can be downloaded to **Android OS** based mobile. Scan QR Code using Code/Bar Scanner from your mobile. (Scanners are available on Google Playstore)